ELSEVIER

Inorganica Chimica Acta 229 (1995) 407–415

Inorganica Chimica Acta

An X-ray determination of the electron distribution in crystals of hexapyridine-*N*-oxide cobalt(II) perchlorate and the electronic structure of the Co^{2+} ion ☆

John S. Wood

Department of Chemistry, University of Massachusetts, Amherst, MA 01002, USA

Received 19 July 1994; revised 29 September 1994

Abstract

The valence electron density distribution in hexapyridine-*N*-oxide cobalt(II) perchlorate, $Co(C_5H_5NO)_6(ClO_4)_2$, has been investigated experimentally using high resolution single crystal X-ray diffraction data collected at 78(1) K with Mo Kα radiation, together with the results from the already reported neutron structure determination. The crystal data at 78 K are $a = 12.317(1)$ and $c = 18.826(1)$ Å; space group $R\bar{3}$, $Z = 3$. Deformation electronic density maps have been calculated from the X-ray data, using parameters from the refinement of the high order data, $\sin\theta/\lambda > 0.75$ Å^{-1}, the parameters obtained from the refinement of the neutron data and from structure factors obtained from a multipole deformation refinement. Conventional spherical atom refinement on 4030 reflections ($F_o \geq 3\sigma F_o$) gives $R = 0.037$ and $R_w = 0.038$, while the multipole refinement on 3627 reflections gives $R = 0.028$ and $R_w = 0.024$. A pronounced aspherical electron distribution has been found for the cobalt atom in the deformation maps which is consistent with a significant trigonal distortion of the distribution expected for an octahedral ligand field, viz. $t_{2g}(5.0)$ and $e_g(2.0)$. The populations obtained from the multipole refinement confirm this and give apparent orbital occupancies of 3.7(1), 1.2(1) and 2.4(1) for the $e_g(t_{2g}^{\pm})$, $a_g(t_{2g}^{0})$ and $e_g'(e_g)$ orbitals respectively, the charge on the cobalt ion being determined as +1.74(4). There is a large e_g–e_g' mixing coefficient which leads to the conclusion that there is a significant departure from the t_{2g} octahedral character of the ground state orbitals. The results are consistent with a ^4A_g ground state for the Co^{2+} ion, which is in accord with the various earlier magnetic, spectroscopic and heat capacity studies.

Keywords: Crystal structures; Electronic structure; Cobalt complexes; Pyridine-*N*-oxide complexes

1. Introduction

The series of hexapyridine-*N*-oxide metallate complexes, $M(C_5H_5NO)_6X_2$ (or $M(PyO)_6X_2$), has been the subject of a variety of physical studies in the last two decades, largely because the electronic properties of the compounds show the presence of large trigonal distortions from those expected for essentially octahedral complexes [1]. These distortions are somewhat unusual, given the near perfect O_h geometry of the MO_6 coordination polyhedra [2,3], but arise primarily because of the non-cylindrical symmetry of the metal–ligand bond and the differences in the π-bonding contributions to the M–O bond, normal to, and in the M–O–N plane. We have previously extensively examined the Jahn–Teller behavior of the copper complexes, [4,5] while others have studied the magnetic anisotropy in the cobalt [6,7] and nickel [8,9] complexes, the Mössbauer spectra of the iron(II) complex, $Fe(PyO)_6(ClO_4)_2$ [10] and the EPR spectra of the manganese doped zinc complex [11]. All of these studies indicate ground state electronic structures for the metal ions corresponding to trigonally elongated octahedra and this has been extensively confirmed in the case of the cobalt complexes ($X = ClO_4$, BF_4, NO_3) using heat capacity measurements to study the low temperature magnetic exchange [12,13]. These measurements reveal that these compounds behave as 3-D XY antiferromagnets, behavior which can only be accounted for assuming a Kramers doublet, $S = \frac{1}{2}$ ground state arising from the ^4A_g ground term.

As part of a program studying electron density distributions in coordination compounds using X-ray dif-

☆ This paper is dedicated to Professor F.A. Cotton on the occasion of his 65th birthday.

SSDI 0020-1693(94)04272-W

fraction measurements, we have accordingly carried out a high resolution, low temperature X-ray study of the cobalt complex, $Co(PyO)_6(ClO_4)_2$, in order to assess the nature and magnitude of the trigonal distortion at the metal atom using this more direct approach, as well as to examine the charge density in the coordinated ligand. A wide variety of high resolution X-ray studies of the electronic structures of transition metal complexes have now been described and for many of these it has proved possible to determine the details of the d-orbital population distribution [14] and in some instances, to resolve uncertainties regarding the assignment of the metal atom ground state [15]. Several octahedral low spin complexes, ML_6, with crystallographically imposed trigonal symmetry (point groups $\bar{3}$ or $\bar{3}m$) have featured in the application of these methods [16,17] and the signs of the trigonal deviations from regular octahedral properties have been determined from the populations of the multipolar functions and found to be in accord with the electronic structures determined indirectly [17,18]. As noted above, although the coordination sphere geometry is essentially perfectly octahedral for the $M(PyO)_6^{2+}$ species, we anticipated that the large trigonal electronic distortions would be observable in the electron density deformation maps and the aspherical atom refinements and the results of the study described in the present paper indicate that this is indeed the case. This analysis uses, in addition, results from our previously reported structure refinement based on neutron data measured at 90 K [19]. Both the neutron structure determination and the analysis of the 78 K X-ray data, described here, reveal that the near perfect octahedral geometry of the coordination polyhedron, found at room temperature, is retained.

2. Experimental

2.1. Sample preparation and data collection

$Co(PyO)_6(ClO_4)_2$ was prepared as described previously [2] and suitable rhombohedral shaped crystals with faces of the form {100} prominent were grown from 95% ethanolic solution. The crystal chosen for data collection was almost equi-dimensional and was mounted on an aluminum pin approximately along the rhombohedral axis. Data were collected on a Picker diffractometer at the Brookhaven National Laboratory, the diffractometer being controlled by locally developed software. Crystal cooling was achieved with a liquid nitrogen cooled cryostat having a beryllium walled chamber [20]. Measurements were made using an ω–2θ step scan technique, the full scan profile of each reflection being analyzed to give the integrated intensity and its standard deviation using PROFILE [21]. The data were collected in shells of increasing sin θ/λ. The six standards used showed a decline in intensity totaling approximately 6% over most of the period of the measurement except for the last shell, for which a more marked decline was observed. Accordingly, only one equivalent for this last shell was measured. The data were corrected for variation in the standards assuming the intensity fall-off to be isotropic and, after correction for absorption, symmetry equivalent reflections were averaged to give 4587 independent data. The contributions of the variation in the standards and the averaging were included in the standard deviations [22]. Complete details of the data collection and processing are given in Table 1.

2.2. Least-squares refinements

Initial coordinates for the refinement models were taken from the neutron structure analysis [19] and in the majority of the calculations, the hydrogen atom coordinates derived from this analysis were used unchanged. Core, valence and total atomic scattering factors for Co, Cl, O, N and C were taken from the International Tables [24] and the hydrogen scattering factor from Ref. [25]. Anomalous scattering was included for all non-hydrogen atoms [26]. The quantity minimized in all refinements was $\Sigma w(|F_o| - k|F_c|)^2$ with $w = 1/\sigma^2(F_o)$.

The principal refinement results for the different structural models are summarized in Table 2 and, apart from a conventional spherical atom refinement utilizing the entire data set, only those reflections having $F_o \geqslant 3\sigma(F_o)$ were used. Hydrogen atom isotropic thermal parameters were determined in the spherical atom refinements based on the data to sin $\theta/\lambda = 1.0$, and were then used together with their neutron coordinates and the parameters for the non-hydrogen atoms obtained from the high angle refinement, in the calculation of the $\Delta\rho(X–X_H)$ deformation density maps. The observed deformation maps, $\Delta\rho(X–X_H)$ and $\Delta\rho(X–N)$, were calculated using the full X-ray data set to a resolution of 1 $Å^{-1}$ and for the calculation of the promolecule density for the (X–N) maps, the neutron thermal parameters were uniformly reduced by 1.18, a factor which to some extent reflects the temperature difference of the X-ray and neutron experiments (see Section 3). The e.s.d. in these maps is calculated to be 0.06 e $Å^{-3}$ except in regions very close to the special positions [27].

In order to describe the aspherical features of the valence density in a more quantitative way, refinement incorporating atom centered density deformation parameters into the least-squares model was undertaken. The multipole expansion model developed by Hansen and Coppens [28] as incorporated in a locally modified version of their program, MOLLY, was used for these refinements. Because of the probable larger errors associated with the reflection data in the region 0.95–1.00

Table 1
Crystal data and data collection details

Compound	$Co(C_5H_5NO)_6(ClO_4)_2$
Unit cell	
a (Å)	12.317(1)
c (Å)	18.826(1)
Z	3
Space group	$R\bar{3}$ (hexagonal setting)
Diffractometer	Picker 4-Circle; Mo Kα radiation; graphite monochromator
λ (Å)	0.71069
Temperature (K)	78(1)
Cell determination	32 reflections in range $35<2\theta\leqslant 45°$
Intensity measurements	$\theta/2\theta$ step scans; step size, 0.04°; reflection widths, 80 to 110 steps
No. reflections	
total measured	12480
index ranges	h and k: −24 to 24; l: 0 to 37
Intensity standards and variation	6 standards including one set of symmetry equivalents; frequency, every 40 reflections; 10% decline in intensity − approximately linear and isotropic
Intensity averaging	
sin θ/λ range Å^{-1}	0.0–0.95, three equivalents
$R(F^2)$(av.), $R_w(F^2)$	0.042, 0.051
sin θ/λ range Å^{-1}	0.95–1.0, one equivalent
total independent reflections	4587
Absorption correction	
crystal size (mm)	0.36×0.44×0.48
faces of form	{1$\bar{1}\bar{1}$} (six) and {001} (two)
absorption coefficient (cm^{-1})	7.57
method	Gaussian integration
transmission coefficients	0.735–0.682
Extinction correction	isotropic secondary extinction parameter refined type I crystal with Lorentzian distribution of mosaicity assumed [23]
extinction parameter	$0.015(2)\times 10^{-4}$
largest correction on F_o	1.07

Table 2
Refinement details for $Co(PyO)_6(ClO_4)_2$

	Spherical atom model		Multipole
Sin θ/λ (Å^{-1})	0–1.0	0.75–1.0	0–0.95
No. reflections, $F_o\geqslant 3\sigma(F_o)$	4030	1329	3627
No. variables	86	81	170[a]
$R(F)$ (all data − 4587)	0.046		
$R(F)$, $F_o\geqslant 3(F_o)$	0.037	0.056	0.028
$R_w(F)$	0.038	0.042	0.024
Goodness-of-fit	3.88	1.18	1.56

[a] Constraints imposed on deformation parameters as follows: C(1)=C(5), C(2)=C(4), H(1)=H(5) and H(2)=H(4). Assumed chemical site symmetries are given in Table 5.

Å^{-1} (vide supra), the multipole refinements were carried out on the data in the region 0.0–0.95 Å^{-1}.

In order to keep the number of parameters to be optimized in the multipole model to a reasonable level, the constraints on the population parameters for chemically equivalent atoms, detailed in Table 2, were imposed and the local chemical site symmetries, given in Table 5, were assumed. The multipole expansion was truncated at the octapolar level ($l=3$) for the ligand atoms (apart from the oxygen, for which $l=4$ functions were included for some refinement cycles) and for the hydrogen atoms a monopole and a single bond directed dipole were included. For the cobalt atom and the perchlorate ion, the expansion included hexadecapolar functions ($l=4$). In addition to the population parameters, the variables κ, which allow for the departure of the spherical Hartree–Fock valence density from the isolated atom value, and $\zeta'(\kappa'\zeta)$, the exponent in the Slater type radial functions used for the multipolar functions, were treated as refinable parameters. In the initial multipole refinements, the cobalt 4s density was included and the population, P_{VAL}, varied. However, this lead to unreasonable values for P_{VAL} and the cobalt ion charge. The diffuse 4s orbital contributes to only a few low angle reflections and refinement gives unreliable estimates of its population. For subsequent calculations, the population was therefore fixed at zero.

Model deformation density maps $\Delta\rho_{model}=(\rho_{model}-\rho_{spherical})$ were calculated using as the structure factors for ρ_{model} those calculated using the final parameters from the multipole refinement, while the spherical atom density was based on parameters from

the high angle refinement. The atomic coordinates from the two refinements differed by no more than two e.s.d.s. Such maps were calculated from structure factors for all the measured data, i.e. sin $\theta/\lambda \leqslant 1.0$ Å^{-1}.

In order to check if the model had satisfactorily fitted the chemically significant features of the experimental density, difference (or residual) density maps, $\rho_{RES} = \rho_{OBS} - \rho_{model}$, were calculated. Apart from the regions around the cobalt and chlorine atoms, which lie on special positions, these maps showed only random noise with peak maxima ~0.1 e Å^{-3}.

3. Results and discussion

It can be seen from the refinement results given in Table 2, that although the R factors for the conventional treatment of the high angle data (sin $\theta/\lambda \geqslant 0.75$ Å^{-1}) are significantly higher than those for the complete data set, the goodness-of-fit index is much lower; the value of near unity indicating that for the high angle reflections, for which the scattering is primarily due to the core electrons, the spherical atom model is much more appropriate. As anticipated, the multipole refinement, on the other hand, results in a significantly better fit to the complete data, than the spherical atom refinement, and the final atomic coordinates resulting from this refinement are given in Table 3. Bond distances and angles are given in Table 4. Fig. 1 illustrates the

Table 3
Fractional coordinates ($\times 10^5$) and equivalent isotropic thermal parameters (Å$^2 \times 10^3$) for $Co(PyO)_6(ClO_4)_2$ at 78 K

Atom	x	y	z	U_{eq} [a]		
				M [b]	H	N
Co	0	0	0	69(1)	83(1)	132(19)
O(1)	15515(7)	10951(8)	6431(4)	120(3)	122(3)	143(5)
N	20575(6)	5288(6)	10004(3)	107(3)	102(3)	129(3)
C(1)	27281(6)	971(7)	6543(4)	143(3)	139(4)	164(5)
C(2)	32588(7)	−4931(7)	10264(4)	168(3)	164(4)	196(5)
C(3)	31116(7)	−6330(7)	17598(4)	175(3)	173(4)	204(5)
C(4)	24317(6)	−1632(7)	21018(4)	161(3)	157(4)	192(5)
C(5)	19135(6)	−4200(6)	17138(4)	130(3)	129(3)	153(5)
Cl	0	0	35013(1)	126(1)	128(2)	162(4)
O(2)	0	0	42637(9)	221(5)	216(5)	279(7)
O(3)	715(6)	−10711(13)	32428(4)	239(5)	233(5)	296(6)
H(1) [c]	2770(2)	224(2)	86(1)	281(15) [d]		361(13)
H(2)	3770(2)	−891(2)	729(1)	315(16)		411(13)
H(3)	3495(2)	−1122(2)	2050(1)	330(16)		429(14)
H(4)	2274(2)	−255(2)	2662(1)	302(16)		401(14)
H(5)	1398(2)	813(2)	1939(1)	270(15)		323(12)

[a] $U_{eq} = \frac{1}{3}\sum_i \sum_j U_{ij} a_i a_j a^*_i a^*_j$.

[b] M = multipole refinement; H = high angle spherical atom refinement; N = neutron values.

[c] The listed coordinates for H(1)–H(5) were obtained from the neutron refinement and used unchanged in the X-ray refinements.

[d] Isotropically refined in multipole refinements.

Table 4
Bond distances and angles in $Co(PyO)_6(ClO_4)_2$ at 78 K [a]

Co–O(1)	2.088(1)		
O(1)–N	1.328(1)		
N–C(1)	1.352(1)	N–C(5)	1.353(1)
C(1)–C(2)	1.386(1)	C(5)–C(4)	1.384(1)
C(2)–C(3)	1.392(1)	C(3)–C(4)	1.391(1)
O(1)–Co–O(1)$_3$	89.75(3)	O(1)–Co–O(1)$_3$	90.25(3)
Co–O(1)–N	118.17(4)		
O(1)–N–C(1)	120.14(5)	O(1)–N–C(5)	118.84(5)
N–C(1)–C(2)	120.25(5)	N–C(5)–C(4)	120.25(5)
C(1)–C(2)–C(3)	119.98(5)	C(3)–C(4)–C(5)	120.09(5)
C(2)–C(3)–C(4)	118.41(6)	C(1)–N–C(5)	121.00(5)
Cl–O(2)	1.435(1)	Cl–O(3)	1.449(1)
O(2)–Cl–O(3)	109.62(3)	O(3)–Cl–O(3)$_3$	109.32(4)

[a] Based on multipole refinement results.

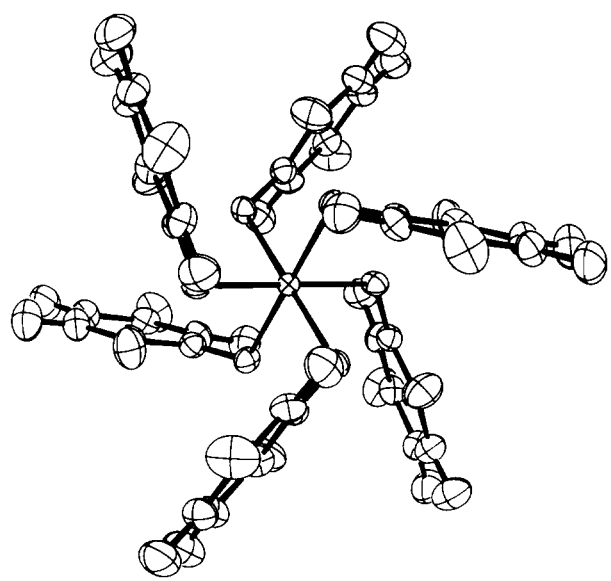

Fig. 1. An ORTEP plot of the $Co(C_5H_5NO)_6^{2+}$ ion viewed down the $\bar{3}$ axis. The thermal ellipsoids are at the 67% probability level and the plot includes the hydrogens as taken from the neutron structure analysis.

structure of the $Co(PyO)_6^{2+}$ cation, including the hydrogens with their thermal motion as determined from the neutron refinement. Also included in Table 3 are the equivalent isotropic thermal parameters derived from the high angle refinement and from the neutron analysis [19]. We see that, apart from the cobalt atom, the U_{eq} for the high angle and multipole refinements differ by only one e.s.d. and comparison of the individual U_{ij} (see Section 5) for the ligand and perchlorate ion atoms shows close similarity for the two refinements. The ratio of U_{eq} and U_{ij} values for the neutron and X-ray refinements reflects the pattern found in earlier studies, namely that the neutron values are systematically larger than those obtained from the X-ray refinement. In the present instance, the ratio of U_{ij}(N)/

U_{ij}(X) for the ligand and ClO_4^- ion, is reasonably constant and reflects quite well the temperature difference (90 versus 78 K) of the two experiments. The neutron values of U_{11} and U_{33} for cobalt however, are in contrast, much larger than those derived from the X-ray refinements, which also differ significantly among themselves. Although their e.s.d.s are large, the neutron results suggest a near isotropic atom, as is also indicated by the multipole refinement.

The high angle refinement gives a more anisotropic atom and the possibility that an anharmonic contribution to the thermal motion might be significant. Such a contribution would be more evident in the high angle data, and although it would also affect the neutron refinement, it might not be detectable, since the cut-off for this data set was 0.66 $Å^{-1}$. However, the asphericity in the 3d density of the cobalt ion could still be having a significant effect in the X-ray data with sin $\theta/\lambda > 0.75$ $Å^{-1}$, since for the later transition metal ions, such as cobalt, the d-orbitals are more contracted and have some core-like character. In this analysis we have assumed this to be the case, and have used the simple harmonic model for the cobalt ion motion.

3.1. Deformation density maps

The observed deformation densities, (X–X_H) and (X–N), calculated in the plane of the ligand, are illustrated in Fig. 2. As observed in many previously reported studies, peaks are found in these maps between all covalently bonded atoms and in the lone pair region of the oxygen atom.

The peak in the N–O bond is significantly lower than those in the ring, in keeping with the general situation for the deformation density for electron rich atoms [29] and as observed for nitropyridine-*N*-oxide [30]. The appearance of the X–X_H map is somewhat superior to that for the X–N map, where the adjustment of the neutron U_{ij} values to the X-ray temperature will introduce uncertainties, particularly at the nuclei.

The deformation density in the region of the cobalt atom forms a puckered hexagonal ring arrangement conforming to the $\bar{3}$ crystal symmetry and Fig. 3 shows cross sections through this distribution in planes containing the Co–O bond and bisecting pairs of bonds. The weak peak maxima in this ring occur at a distance of ~0.6 Å from the cobalt and they lie between the bond directions and approximately towards the centers of six of the faces of the CoO_6 octahedron. This is consistent with the preferential occupation of the t_{2g} orbitals in the cobalt atom. However, the two additional peaks expected for completion of the t_{2g} set and which would be located on the three-fold axis, are absent. These qualitative results are then indicative of a strong trigonal distortion, in which the e_g orbitals (in S_6 symmetry) of t_{2g} parentage, are preferentially occupied

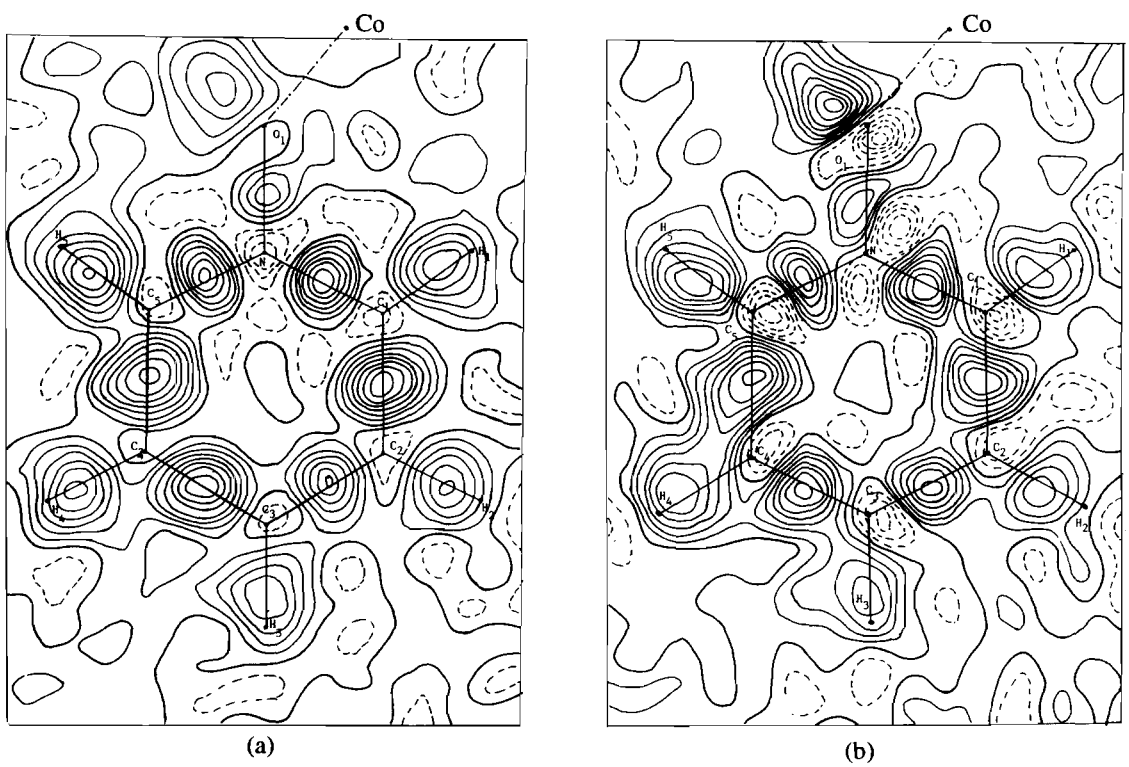

Fig. 2. Observed deformation densities in the plane of the pyridine-*N*-oxide ligand. (a) The (X–X_H) density map and (b) the (X–N) density map. Contours are at 0.10 e $Å^{-3}$ intervals with negative contours dashed. The projection of the Co–O bond vector onto the ligand plane is indicated.

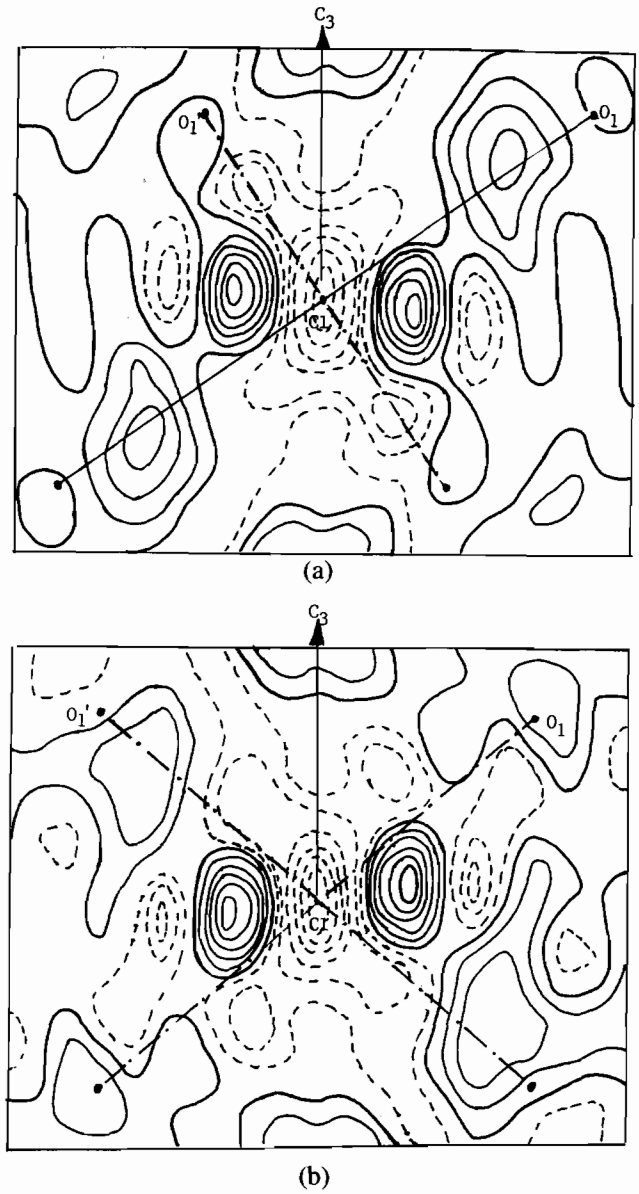

Fig. 3. Observed ($X-X_H$) deformation density maps for planes containing the cobalt atom and the crystallographic C_3 axis. Plot (a) contains the Co–O bond vector and plot (b) is the plane bisecting pairs of Co–O bonds. This plane is orthogonal to the plane in plot (a). The projected positions of the Co–O bonds not in the planes are indicated by the dot-dash lines. Contours are as in Fig. 2.

with respect to the a_g orbital, and this population difference is quantitatively confirmed by the multipole analysis. Fig. 4 shows an ($X-X_H$) deformation map for a section through the perchlorate ion.

3.2. Multipole refinements

The parameters resulting from the multipole refinement are given in Table 5, see also Section 5. The multipole populations for the ligand ring atoms appear to be typical of those for trigonal sp^2-type atoms in aromatic systems, and Fig. 5(a) shows a model deformation density map for the ligand plane calculated with the final parameters. The electron density maxima in this map are somewhat higher than those in the experimental ($X-X_H$) map, and particularly so for the N–O bond region, but otherwise the bonding and lone pair region features are rather similar. The charge distribution for the ligand leads to an overall charge of −0.06(5), i.e. an essentially neutral ligand. The

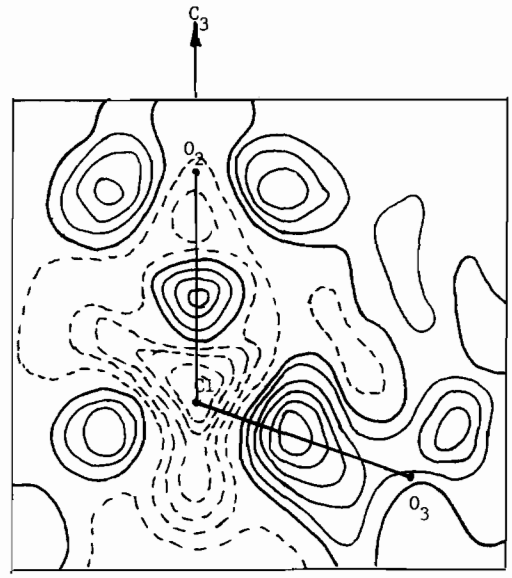

Fig. 4. Observed ($X-X_H$) deformation density map for the perchlorate ion in the plane containing the crystallographic C_3 axis and the Cl–O(3) bond. The contours are as in Fig. 2.

Table 5
Monopole populations (P_{VAL}) and radial exponents for $Co(PyO)_6(ClO_4)_2$

Atom	Assumed site symmetry	P_{VAL}	Charge	κ
Co	$S_6(\bar{3})$ [a]	7.26(6) [b]	+1.74	0.935(5) [c]
O(1)	C_s	6.83(4)	−0.83	0.955(3)
N	C_{2v}	4.73(6)	+0.27	1.015(6)
C(1) [d]	C_s	4.26(5)	−0.26	0.983(5)
C(2) [d]	C_{2v}	4.27(5)	−0.27	
C(3)	C_{2v}	4.12(5)	−0.12	
Cl	C_{3v} [e]	7.12(3)	−0.12	0.996(7)
O(2)	C_{3v} [e]	6.10(4)	−0.10	1.008(4)
O(3)	C_{3v}	6.21(3)	−0.21	
H(1) [d]	$C_{\infty v}$	0.68(3)	+0.32	1.26(4)
H(2) [d]	$C_{\infty v}$	0.63(3)	+0.37	
H(3)	$C_{\infty v}$	0.70(3)	+0.30	

[a] Crystal site symmetry.

[b] For the cobalt atom this is the P_{00} term of the multipole deformation functions, the other non-zero terms are as follows: P_{20}, −0.61(4); P_{40}, 0.27(4); P_{43+}, −0.07(3) and P_{43-}, −0.05(3). The z axis of the local coordinate system lies along the three-fold axis and x lies in the plane containing the Co–O bond and the C_3 axis.

[c] κ for cobalt applies to the deformation functions noted above, and gives a radial exponent $\zeta = 7.39(4)$ a.u.$^{-1}$.

[d] Constraints applied according to Table 2.

[e] Crystal site symmetries for these atoms is $C_3(3)$.

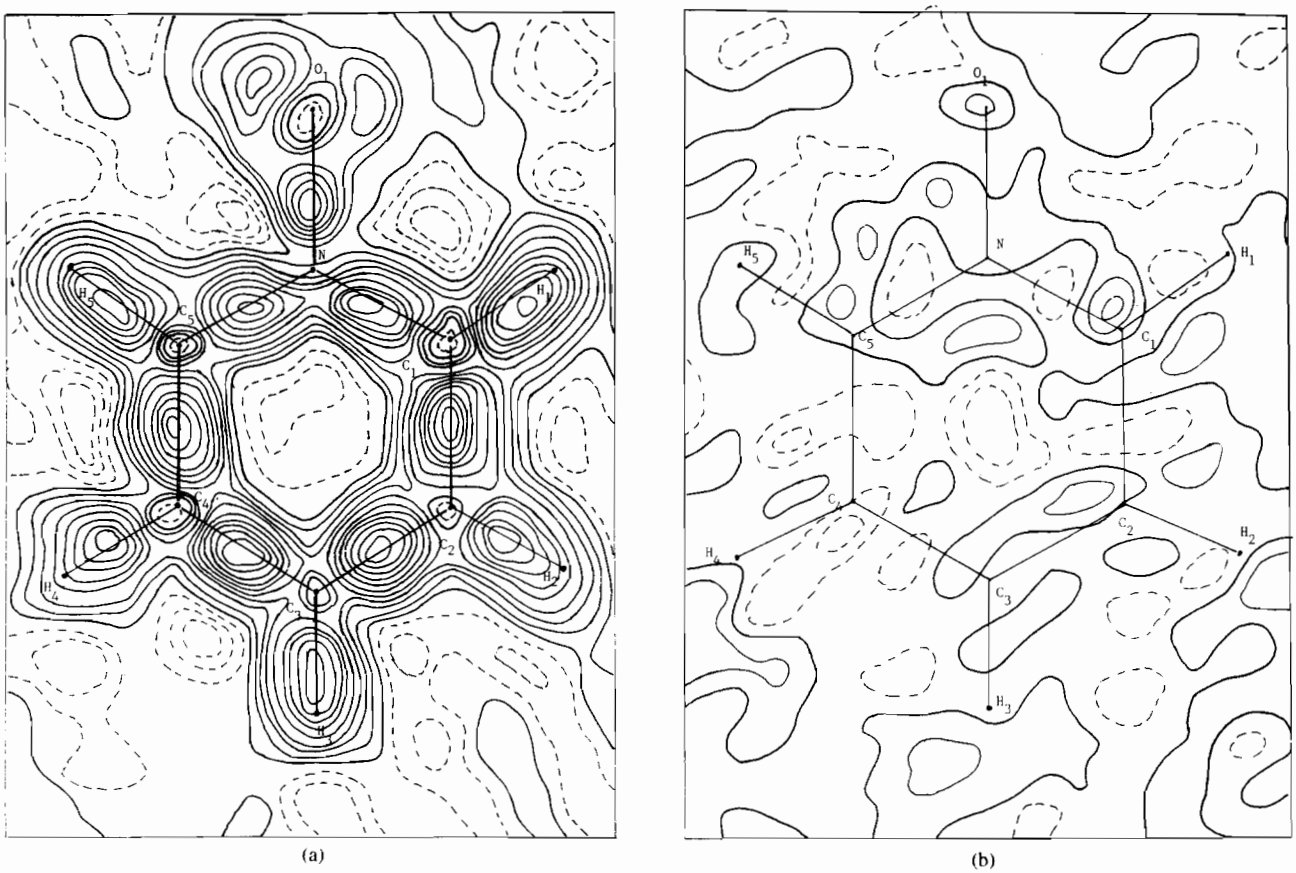

Fig. 5. Plot (a) shows the model deformation density map for the plane of the pyridine-*N*-oxide ligand calculated using structure factors based on parameters from the multipole refinement, while plot(b) shows the residual density map for the same plane. The contours in both maps are as in Fig. 2.

oxygen donor atom, however, carries quite a large negative charge, and this appears to be generally true for the ligand donor atoms in other transition metal species that have been studied by this method [31]. The residual density map for the ligand plane given in Fig. 5(b), exhibits only random noise and indicates that the multipole model gives a good description of the charge density.

The total charge on the perchlorate ion is effectively −1.0 and is uniformly distributed over the ion. Refinement constraining the multipole parameters of O(2) and O(3) to be the same and assuming Cl has T_d chemical site symmetry, was only marginally inferior to the less symmetrical model. The dipole value for hydrogen H(2), and by constraint H(3), is close to zero in contrast to those for H(1) (and H(5)) and H(3). This low value seems to be in accord with the rather strong C–H···O hydrogen bonding involving H(2) and the O(3) atom of the perchlorate [19].

Turning to the cobalt ion, the P_{VAL} value of 7.26(6) leads to a charge of +1.74 in good agreement with the formal oxidation state for the ion. Since in the final cycles of refinement the 4s orbital was assumed to have zero occupancy, this may influence the metal charge somewhat. The values of the allowed multipole function populations, P_{20}, P_{40}, P_{43+} and P_{43-} are given in Table 5, footnote (b). These values differ from those obtained in the earlier studies of the low spin trigonally distorted octahedral systems, where the increased occupancy of the e_g component of the t_{2g} orbitals relative to the upper e_g set, is reflected mostly in the negative value of the population of the P_{43+} (or P_{43-}) multipole function [17,18] [1]. In the present case, P_{20} is the significant multipole and the relatively large and negative value is indicative of the depopulation of the $a_g(d_{z^2})$ orbital relative to the e_g component of t_{2g}. In this instance, the values of P_{43+} and P_{43-} are small and similar in magnitude. Rotating the x and y components of the local coordinate system, which has a Co–O bond direction in the xz plane, by ~12° eliminates the P_{43-} component and gives a revised value, P'_{43+}, of −0.086(20). This rotation is consistent with the observation that the six weak maxima in the near continuous ring of deformation density around the cobalt

[1] Based on the reported orbital populations given for $Co(NH_3)_6Cr(CN)_6$ and $Co(NH_3)_6Co(CN)_6$, in Table 11 of Ref. [18], the signs of the multipole population parameters given in Table 6, appear to be incorrect.

ion, seen in the $X-X_H$ map, are not directed exactly into the faces of the octahedron, as would be expected for the density arising from equally populated t_{2g} orbitals. This, together with the absence of a_g deformation density peaks, suggests that the compositions of the t_{2g} and e_g orbitals in the $\bar{3}$ symmetry are significantly different from those in O_h and this is confirmed quantitatively.

In order to calculate the individual d-orbital occupancies, we used the familiar octahedral basis set quantized along the three-fold axis, namely $a_g = (z^2)$, $e_{g+} = (2/3)^{1/2}(x^2-y^2) - (1/3)^{1/2}(xz)$, $e_{g-} = (2/3)^{1/2}(xy) + (1/3)^{1/2}(yz)$, $e'_{g+} = (1/3)^{1/2}(x^2-y^2) + (2/3)^{1/2}(xz)$ and $e'_{g-} = (1/3)^{1/2}(xy) - (2/3)^{1/2}(yz)$, together with the orbital–multipole relations for this basis given by Coppens and co-workers [18]. The multipole populations then give orbital occupancies: $P_1(a_g) = 1.19(8)$, $P_2(e_g) = 3.62(8)$ and $P_3(e'_g) = 2.44(8)$, based on the total d-orbital occupancy (P_{00}) of 7.26 e. Comparing these values with the populations expected for the high spin octahedrally distributed d^7 configuration, namely $a_g(1.67)$, $e_g(3.34)$ and $e'_g(2.0)$, we see that within the octahedral basis, they are consistent with a trigonal distortion in which the $e_g^{\pm}$ orbitals are stabilized relative to a_g, and that since the a_g population is much lower than expected for O_h symmetry, the distortion is quite large. A measure of the magnitude of the distortion may be obtained from the e_g–e'_g mixing population parameter P_4 [2] which, in the present case, has the rather large value of 2.26. Since the e_g and e'_g orbitals belong to the same representation, we can write the new linear combinations, $\phi_1(e_g^{(a)}) = C_1(e_{g\pm}) + C_2(e'_{g\pm})$ and $\phi_2(e_g^{(b)}) = C_2(e_{g\pm}) - C_1(e'_{g\pm})$ and use the cross term P_4 to evaluate C_1 and C_2. These have the values 0.93 and 0.36, respectively, and lead to revised wave functions, $\phi_1(e_{g+}^{(a)}) = 0.965(x^2-y^2) - 0.26(xz)$ and $\phi_1(e_{g-}^{(a)}) = 0.965(xy) + 0.26(yz)$, for the lower energy set. These have a significantly different composition from the octahedral orbitals. Using the multipole populations, revised occupancies can then be evaluated for the above orbitals, and using $P_{00} = 7.26$ as before, these are $P_1(a_g) = 1.19(8)$, $P_2(e_g^{(a)}) = 4.04(8)$ and $P_3(e_g^{(b)}) = 2.03(8)$, or essentially, $e_g^4 a_g^1 e_g^2$ for the d^7 configuration. The most stable orbitals then are much closer in character to 'pure' $d_{x^2-y^2}$ and d_{xy} (and the least stable to d_{xz} and d_{yz}) and their near integer value populations suggest that only one configuration contributes significantly to the ground state, which is therefore confirmed as ^4A_g. In addition, there seems to be little evidence for the covalent interactions between the cobalt and ligand orbitals, which should also result in non-integral occupancies [14].

The refined ζ value for the cobalt is in a reasonable range for 3d electrons. The value of 3.70(4) a.u.$^{-1}$ corresponds to a slightly expanded d-shell compared with the optimized single Slater exponent of 3.95 a.u.$^{-1}$ for the neutral atom [32]. Normally a somewhat contracted value might be expected since the cobalt carries a positive charge. However, as noted earlier, since the diffuse 4s density has been neglected in the refinement, this may be compensated for, both in the valence population and the κ value.

[2] The contribution to the electron density arising from the mixing of e_g and e'_g orbitals is given by $\frac{1}{2}P_4(e_{g+}e'_{g+} + e_{g-}e'_{g-})$: see Eq. (3) of Ref. [18].

4. Conclusions

The d-electron distribution for the cobalt ion in $Co(C_5H_5NO)_6(ClO_4)_2$ has been determined from low temperature X-ray diffraction measurements and it has proved possible to observe directly the effect of the electronic trigonal distortion of the octahedral ligand field. The derived orbital occupancies give an electronic ground state of ^4A_g for the ion and the sign of the distortion, i.e. as a trigonal elongation, is consistent with the results of a variety of indirect spectroscopic and magnetic measurements. Although the coordination polyhedron is octahedral, the distortion is quite large and it has proved possible to derive 'revised' ground state orbitals from the multipole refinement parameters.

5. Supplementary material

Lists of U_{ij} values, multipole refinement parameters, and Tables of structure factors are available from the author on request.

Acknowledgements

I am indebted to Dr R.K. Brown and Dr. F. Takusagawa for their assistance with the low temperature X-ray data collection.

References

[1] R.L. Carlin and A.J. van Duyneveldt, *Magnetic Properties of Transition Metal Compounds*, Springer, New York, 1977, p. 234.
[2] T.J. Bergendahl and J.S. Wood, *Inorg. Chem.*, *14* (1975) 338.
[3] D. Taylor, *Aust. J. Chem.*, *31* (1978) 713.
[4] J.S. Wood, C.P. Keijzers, E. de Boer and A. Buttafava, *Inorg. Chem.*, *19* (1980) 2213.
[5] C.P. Keijzers, R.K. McMullan, J.S. Wood, G. van Kalkeren, R. Srinivasan and E. de Boer, *Inorg. Chem.*, *21* (1982) 4275.
[6] D.J. Mackey, S.V. Evans and R.F. McMeeking, *J. Chem. Soc., Dalton Trans.*, (1978) 160.
[7] R.L. Carlin, C.J. O'Connor and S.N. Bhatia, *J. Am. Chem. Soc.*, *98* (1976) 685.

[8] R.L. Carlin, C.J. O'Connor and S.N. Bhatia, *J. Am. Chem. Soc., 98* (1976) 3523.
[9] D.J. Mackey and R.F. McMeeking, *J. Chem. Soc., Dalton Trans.,* (1977) 2186.
[10] G.H.M. Calis, A.E.M. Swolfs and J.M. Trooster, *Chem. Phys., 64* (1982) 259.
[11] C.J. O'Connor and R.L. Carlin, *Inorg. Chem., 14* (1975) 291.
[12] H.A. Algra, L.J. de Jongh, W.J. Huiskamp and R.L. Carlin, *Physica B (Amsterdam), 83B* (1976) 71.
[13] J. Bartolome, H.A. Algra, L.J. de Jongh and R.L. Carlin, *Physica B&C (Amsterdam), 94B* (1978) 60.
[14] B.N. Figgis, L. Khor, E.S. Kucharski and P.A. Reynolds, *Acta Crystallogr., Sect. B, 48* (1992) 144.
[15] P. Coppens, L. Li and N.J. Zhu, *J. Am. Chem. Soc., 105* (1983) 6173; N. Li, Z. Su, P. Coppens and J. Landrum, *J. Am. Chem. Soc., 112* (1990) 7294.
[16] M. Iwata, *Acta Crystallogr., Sect. B, 33* (1977) 59; M. Iwata and Y. Saito, *Acta Crystallogr. Sect. B, 29* (1973) 822.
[17] E.D. Stevens, M.L. DeLucia and P. Coppens, *Inorg. Chem., 19* (1980) 813.
[18] A. Holladay, P. Leung and P. Coppens, *Acta Crystallogr., Sect. A, 39* (1983) 377.
[19] J.S. Wood, R.K. Brown and M.S. Lehmann, *Acta Crystallogr., Sect. C, 42* (1986) 410.
[20] P. Coppens, F.K. Ross, R.H. Blessing, W.F. Cooper, F.K. Larsen, J.G. Leipoldt, B. Rees and R. Leonard, *J. Appl. Crystallogr., 7* (1974) 315.
[21] R.H. Blessing, P. Coppens and R. Becker, *J. Appl. Crystallogr., 7* (1974) 488.
[22] L.E. McCandlish, G.H. Stout and L.C. Andrews, *Acta Crystallogr., Sect. A, 31* (1975) 245.
[23] P. Becker and P. Coppens, *Acta Crystallogr., Sect. A, 31* (1974) 417.
[24] *International Tables for X-ray Crystallography*, Vol. 4, Kynoch, Birmingham, UK, 1974.
[25] R.F. Stewart, R.F. Davidson and W.T. Simpson, *J. Chem. Phys., 42* (1965) 3175.
[26] D.T. Cromer and D.J. Liberman, *J. Chem. Phys., 53* (1970) 1891.
[27] D.W.J. Cruickshank, *Acta Crystallogr., 2* (1949) 65.
[28] N.K. Hansen and P. Coppens, *Acta Crystallogr., Sect. A, 34* (1978) 909.
[29] J.D. Dunitz and P. Seiler, *J. Am. Chem. Soc., 105* (1983) 7056.
[30] P. Coppens and M.S. Lehmann, *Acta Crystallogr., Sect. B, 32* (1976) 1777.
[31] E.D. Stevens, *J. Am. Chem. Soc., 103* (1981) 2982; C.L. Lecomte, D.L. Chadwick, P. Coppens and E.D. Stevens, *Inorg. Chem. 22* (1983) 2982.
[32] E. Clementi and D.L. Raimondi, *J. Chem. Phys., 38* (1963) 2686.